THE JOURNAL OF PHYSICAL CHEMISTRY B

ARTICLE

pubs.acs.org/JPCB

β-Phase Formation of Poly(9,9-dioctylfluorene) Induced by Liposome Phospholipid Bilayers

María José Tapia,[*,†] María Monteserín,[†] Hugh D. Burrows,[*,‡] J. Sérgio Seixas de Melo,[‡] João Pina,[‡] Ricardo A. E. Castro,[§] Sonia García,[∥] and Joan Estelrich[∥]

[†]Departamento de Química, Universidad de Burgos, Plaza Misael Bañuelos, Burgos 09001, Spain

[‡]Departamento de Química, Universidade de Coimbra, 3004-535 Coimbra, Portugal

[§]Faculdade de Farmácia, Universidade de Coimbra, 3000-548 Coimbra, Portugal

[∥]Facultat de Farmàcia, Universitat de Barcelona, Avda. Joan XXIII s/n 08028 Barcelona, Catalonia, Spain

Supporting Information

ABSTRACT: The well-structured β-phase emission of the neutral poly(9,9-dioctylfluorene) (PFO) is observed in 1,2-dimyristoyl-*sn*-glycero-3-phosphocholine (DMPC) bilayers, either as polydisperse aqueous liposomes or as the lamellar phase in thin films, and has been characterized by absorption, fluorescence (steady-state and time-resolved), and fluorescence anisotropy spectroscopy. Inclusion of PFO in DMPC liposomes provides a way of obtaining the ordered structure of this neutral polymer in aqueous suspensions. Quantification of the increase of the PFO β-phase in DMPC liposomes with the increase in polymer concentration is followed by deconvolution of the absorption spectra. In solid films, the presence of the phospholipids enhances the β-phase formation. In addition, the effect of the PFO concentration on the phospholipid phase transitions has been studied by differential scanning calorimetry (in liposome) and polarized light thermal microscopy (in solid film), confirming PFO/DMPC interactions in both liposome and films. The liposome size and structure in the presence and absence of polymer were characterized by dynamic light scattering and transmission electron microscopy, which showed relatively modest changes in liposome shape but a decrease in size upon incorporation of PFO.

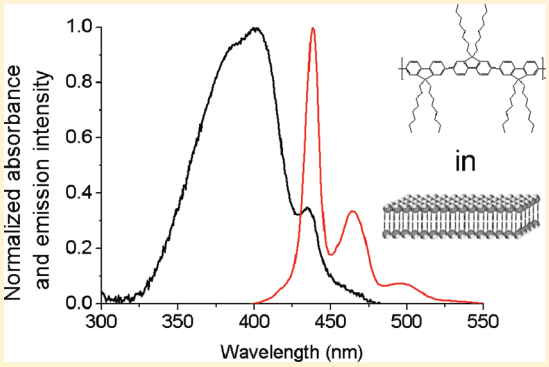

INTRODUCTION

Poly(9,9-dioctylfluorene) (PFO, Figure 1) is a blue emitting polymer widely used in polymer light-emitting diodes (PLEDs),[1−5] photovoltaics cells,[6−8] or lasers.[9−16] Recently, the combination of the blue light emission of PFO with the deep level emissions from ZnO nanorods[1] or CdSe−ZnS quantum dots[2] has allowed the fabrication of white light LED. Much attention has focused on PFO since it shows a variety of secondary structures, depending on factors such as solvent and temperature, which can modify its photophysical behavior.[17−19] Particular emphasis has focused on the so-called β-phase, which shows enhanced luminescence, a characteristic well-defined narrow absorption band at 438 nm, and an unusually well-resolved fluorescence.[20] Random conformational domains (represented by α) and the more planar β-phase normally coexist, and efficient energy migration occurs from disordered regions to the β-conformation.[20] The enhanced optoelectronic properties resulting from β-phase formation can arise from interchain ordering, crystallization,[17] or aggregation[20] and potentially have major technological applications, including organic lasers[12] with spatial control of lasing wavelength through patterning in a glassy PFO film coated on a one-dimensional distributed-feedback grating etched into a substrate.[9] However, the mechanism leading to the formation of the β-phase is not completely understood.[19] While it is not clear whether β-phase formation can occur in single chains[21] or requires aggregation, an increasing body of evidence suggests that interactions involving alkyl side chains on PFO are involved in β-phase formation,[22,23] and the investigation of novel systems in which this ordered phase is formed is likely to provide valuable insights into its formation mechanism. We describe the phospholipid induced formation of β-phase in aqueous suspensions of PFO incorporated into 1,2-dimyristoyl-*sn*-glycero-3-phosphocholine (DMPC, Figure 1), either as liposomes or liquid crystals. The combination of a wide range of experimental techniques allows us to get a broad picture of both the changes in the spectroscopic properties of PFO (absorption and emission spectra) and the structural changes in the phospholipids, phase transitions (differential scanning calorimetry, DSC, and polarized light thermal microscopy, PLTM), liposome sizes (dynamic light scattering, DLS), and liposome shapes (transmission

Received: February 1, 2011
Revised: April 6, 2011
Published: April 26, 2011

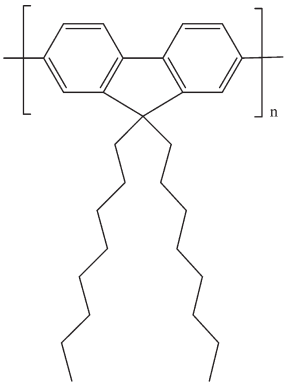

PFO

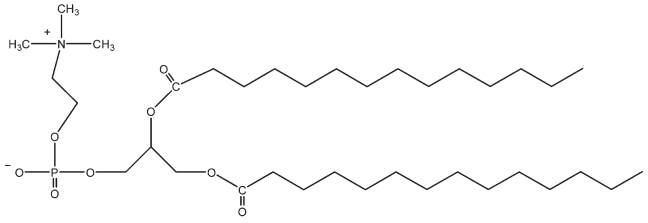

DMPC

Figure 1. Poly(9,9-dioctylfluorene) (PFO) and 1,2-dimyristoyl-*sn*-glycero-3-phosphocholine (DMPC) structures.

electron microscopy, TEM), with the increase of PFO/phospholipid ratio. In addition to its relevance on the driving force for β-phase formation, this may also provide a valuable fluorescent probe of phospholipids, including actual biological membrane bilayers.

EXPERIMENTAL METHODS

1.1. Materials and Sample Preparation. 1,2-Dimyristoyl-*sn*-glycerol-3-phosphatidylcholine (DMPC) and poly(9,9-dioctylfluorene) (PFO, stated M_n = 15.8 kg/mol, M_w = 58.2 kg/mol) were purchased from Sigma and used without further treatment (Figure 1). Trizma (pH = 7.4) buffer solution was prepared with Trizma Base (Sigma) and HCl 37% (Panreac).

Liposomes were prepared by the thin film hydration method. DMPC and DMPC−PFO mixtures in chloroform were evaporated to dryness by bubbling argon. The resulting films were hydrated with Trizma−HCl buffer solution (pH = 7.4) to obtain a final DMPC concentration around 9×10^{-5} M and PFO concentrations from 1×10^{-6} to 1×10^{-5} M (except in DSC experiments, on which DMPC concentration is around 4×10^{-2} M and PFO concentrations range from 1×10^{-3} to 4×10^{-2} M).

To form liposomes, the samples were kept at 40 °C for 10 min (temperature above the DMPC gel−liquid crystalline phase transition) and then vortexed three times for 1 min. They were then alternatively sonicated and heated to 40 °C, for 5 min each, during 1 h. The samples were then kept at 40 °C while stirring for another hour.

Drop-cast films were prepared by evaporating chloroform of solutions containing the appropriate PFO/DMPC ratio on sapphire discs.

1.2. Apparatus and Methods. Absorption spectra were recorded on a Shimadzu 2501 PC UV−visible spectrophotometer. Steady-state luminescence spectra used a Shimadzu RF-5301 PC fluorimeter, with 387 nm excitation, 3 and 1.5 nm excitation, and emission slits, with spectra recorded at 25.00 °C ± 0.01 °C. Emission spectra of thin films were obtained using a Horiba−Jobin−Yvon integrating sphere.

Time-resolved fluorescence measurements used single photon counting with picosecond time resolution on a previously described apparatus,[24] exciting at 392 nm, with emission observed at 440, 465, and 500 nm. Fluorescence decays and the instrumental response function (IRF) were collected using 4096 channels (0.814 ps/ch), until 5×10^3 total detected counts at maximum were reached. Deconvolution of fluorescence decay curves used the method of the modulation functions previously implemented by G. Striker.[25]

Polarized fluorescence spectroscopy experiments were made, with the fluorescence anisotropy calculated according to eq 1[26]

$$\langle r \rangle = \frac{I_{VV} - GI_{VH}}{I_{VV} + 2GI_{VH}} \quad (1)$$

where $I_{ex,em}$ is the intensity of the emission; V and H are the vertical or horizontal alignment of the excitation and emission polarizers; and $G = I_{HV}/I_{HH}$ is the instrumental correction factor.

These experiments were carried out with a polarization setup consisting of two Glan−Thompson rotatable prism polarizers. The single channel (L-format) method for fluorescence anisotropy determination was used. To calculate each anisotropy value via eq 1, four complete fluorescence spectra, one for every configuration of polarizers, were required. The fluorescence spectra, for anisotropy experiments, were recorded on a Jobin−Yvon Fluorolog 3.2.2 spectrometer with right angle geometry, exciting at 387 nm, with excitation and emission slits of 0.5 mm.

Dynamic light scattering (DLS) measurements were carried out using a Zetasizer Nano ZS90 (Malvern, UK) to determine the hydrodynamic diameter and the polydispersity index (PI) of the liposomes. The DLS technique measures the Brownian motion of the particles and correlates it with the hydrodynamic radius, r_h, of a particle defined by the Stokes−Einstein equation

$$r_h = \frac{kT}{3\pi\eta D} \quad (2)$$

where D is the translational diffusion coefficient (m^2/s); k is the Boltzmann constant; T is the absolute temperature (K); and η is the coefficient of viscosity (Pa s). A 632 nm He/Ne laser beam crosses the sample, and the scattered light at 90° is analyzed considering the size distribution by intensity and by volume of scattered light. The DLS measurements were performed at 25 °C.

Differential scanning calorimetry (DSC) measurements were performed on a MDSC Q-200 TA differential scanning calorimeter equipped with a refrigerated cooling system (RCS). A 50 mL/min Nitrogen purging gas flow was used. The samples were initially cooled to −2 °C and pre-equilibrated at this temperature for 30 min. Three heating−cooling cycles between −2 and 60 °C with a heating rate of 1.5 °C/min were carried out with each sample, obtaining a very good reproducibility between consecutive scans.

For transmission electron microscopy (TEM), liposomes were observed using a Tecna SPIRIT microscope (FEI-company, Netherlands), operating at 120 kV. Samples were prepared by placing a drop of liposome dispersion onto a 400-mesh copper grid coated with carbon film with a Formvar membrane. After staining with uranyl acetate, these were allowed to dry in air before observation. Images were recorded with a Megaview III camera, with data acquisition using Olympus iTEM Soft-Imaging software.

dx.doi.org/10.1021/jp2010666 |J. Phys. Chem. B 2011, 115, 5794–5800

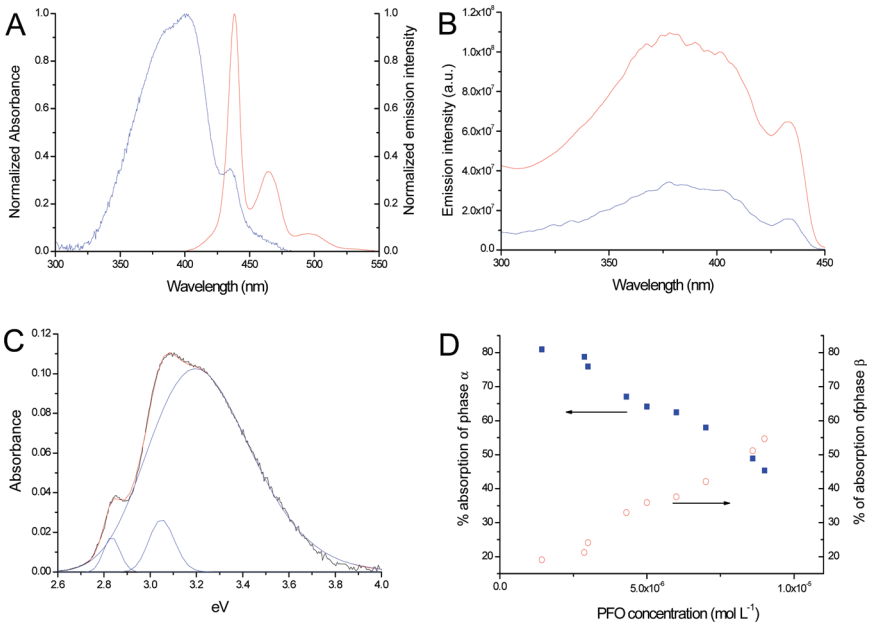

Figure 2. (A) Normalized corrected absorption and emission spectra of PFO 1.40×10^{-5} M in aqueous liposome suspensions of DMPC (9.35×10^{-5} M) in blue and red lines, respectively. (B) Excitation spectra with 465 nm emission wavelength of PFO 4.62×10^{-6} M (blue line) and 8.32×10^{-6} M (red line) in DMPC (9.35×10^{-5} M). (C) Experimental absorption spectrum of PFO 1.40×10^{-5} M in aqueous suspensions of liposomes with DMPC 9.35×10^{-5} M (black line). Calculated absorption spectrum (red line) and its deconvolution into three Gaussians (blue lines). (D) Percentages of absorption of α (blue squares) and β (red circles) phases versus PFO concentration.

Polarized light thermal microscopy (PLTM) studies used a Linkam hot stage, model DSC600, a Leica DMRB microscope, and a Sony CCD-IRIS/RGB video camera. Linkam Real Time Video Measurement System software was used for image analysis. The samples were observed using a water penetration technique. In this technique, the sample is placed on the slide and near is put small pieces of broken glass. The coverslip is placed first over the sample and dropped onto the pieces of broken glass. A small drop of water is placed in the space created by the pieces of broken glass. A boundary between water and the sample is created and observed under partially crossed polarizers, using a 200× magnification.

RESULTS AND DISCUSSION

Spectroscopy. PFO is a neutral polymer (Figure 1) which can only be taken into aqueous systems through interaction with amphiphiles, such as phospholipids, as has previously been indicated for the neutral poly[9,9-bis(6′-bromohexyl)-2,7-fluorene-co-alt-1,4-phenylene], $PFPBr_2$, in DMPC liposomes.[27]

Normalized corrected absorption and emission spectra of PFO in DMPC liposomes are shown in Figure 2A. Scattering background from the liposomes was corrected by subtracting the apparent absorption of free liposomes from those with PFO, normalized at 500 nm. With the corrected PFO absorption spectra in liposomes (Figures 2A, 2C), both the characteristic α-phase band at 387 nm and the β-phase absorption at 438 nm are observed. However, in the emission spectra, only the PFO β-phase emission is seen (Figure 2A). In agreement with previous studies,[20] this indicates efficient energy transfer from the α- to β-phase, which is supported by the excitation spectra of PFO in liposome for emission at 465 nm (Figure 2B) closely resembling the absorption spectra.

The PFO absorption and emission intensities at 405 and 439 nm, respectively, at constant phospholipid concentration grow linearly with the PFO molar concentration between 2×10^{-6} M and 1×10^{-5} M (in terms of repeat units; Supporting Information, Figure S1). Below this range of concentrations, the emission is not observed, while above 10^{-5} M, the linearity is lost, probably due to reabsorption.

The increase of the β-phase contribution to the total absorption of PFO in liposomes upon increasing PFO concentration was followed by deconvolution of the absorption spectra into three Gaussians (using Origin 7.5), attributing that at 379 ± 1 nm (3.27 eV) to the absorption of α-phase and those at 404 ± 2 nm (3.07 eV) and 435 ± 1 nm (2.92 eV) to the absorption of the β-phase, as shown in Figures 2C and 2D.

A linear correlation was found between the increase of percentage of β-phase and the increase of the number of PFO chains per liposome calculated considering the experimentally determined liposome radius (Figure S2 in the Supporting Information), indicating that polymer−polymer interaction plays a role in the formation of the β-phase.

Further information was obtained from the concentration dependence of PFO time-resolved fluorescence in DMPC−PFO solutions (Figure 3). The decays collected at 440 and 500 nm were best fitted by sums of two exponentials (with decay times τ_i and pre-exponential factors a_i). The decay times, 116 ± 14 and 247 ± 25 ps, are characteristic of the β-phase emission, as previously described by Dias et al. (130 and 270 ps)[20] for PFO β-phase in methylcyclohexane (MCH). These short decay times are suggested to arise from ordered chain domains with longer conjugation lengths than the disordered α-phase conformations in the same solvent (τ = 340 ps).[20]

Interaction of PFO with DMPC (either in liposomes or DMPC-water lamellar liquid crystals, data not shown) induces the formation of the β-phase even for low PFO concentrations.

dx.doi.org/10.1021/jp2010666 |J. Phys. Chem. B 2011, 115, 5794–5800

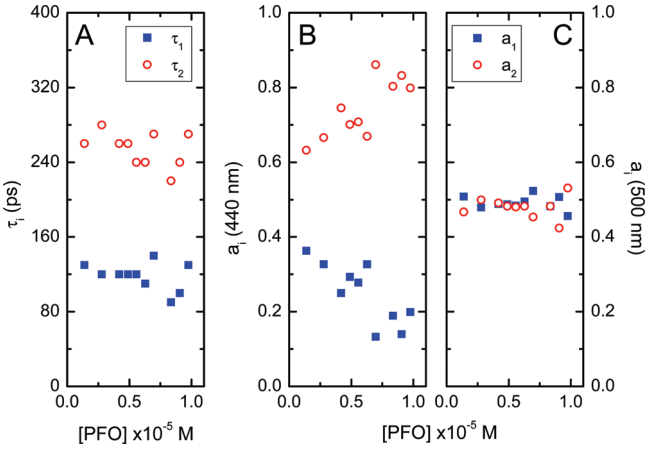

Figure 3. Concentration dependence of the fluorescence decay times, λ_{exc}= 392 nm (A), and pre-exponential factors at λ_{em} = 400 nm (B) and 500 nm (C) of PFO in DMPC (9.56×10^{-5} M)−PFO solutions (in Trizma−HCl buffer). The decays were obtained using global analysis.

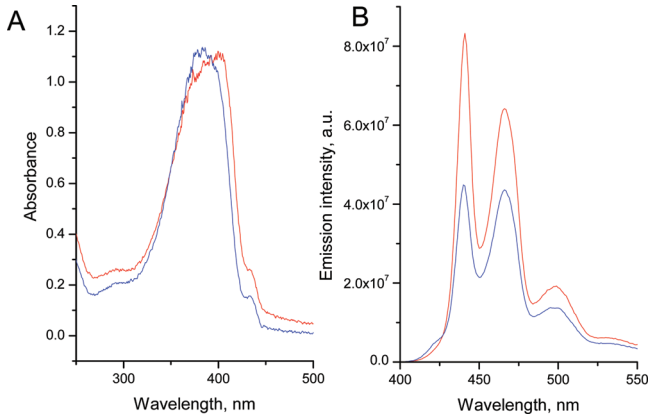

Figure 4. Absorption (A) and emission (B) spectra of drop cast films of PFO (9.63×10^{-6} M, blue line) and of PFO (6.42×10^{-6} M)−DMPC (1.63×10^{-6} M, red line).

Upon increasing PFO concentration in the liposomes, the contribution of the longest component (247 ps) to the total emission ($a_i\tau_i/\Sigma_{i=1}^{2} a_i\tau_i$) is enhanced, while that from the shorter component (116 ps) decreases (Figure 3).

Although the lifetimes of PFO in liposomes are close to those for its β-phase in MCH, the PFO fluorescence anisotropy upon exciting the α-phase in liposome at 387 nm is close to zero (Figure S3, Supporting Information), while that reported in MCH upon exciting at 384 is 0.11.[20]

Loss in fluorescence anisotropy in liposomes may stem from three different mechanisms: rotational diffusion,[26] exciton migration, and conformational relaxation (twisting of part of the aromatic backbone).[28] With the polymer enclosed in liposomes, the third mechanism is unlikely (which is further confirmed by the absence of a rising component at any emission wavelength, Figure 3), and the rotational diffusion of liposomes will be relatively slow, such that exciton migration between close polymer chains in the same liposome is the most likely mechanism to explain the loss of anisotropy, showing that more than one PFO is present in each liposome.

To gain insight into the role the phospholipid vesicles play in the PFO β-phase formation, the absorption and emission spectra of films of PFO and PFO with DMPC drop-cast from chloroform (Figure 4) were registered. Although in both cases the spectroscopic characteristics of the β-phase are observed (narrow absorption peak at 437 nm and a well-resolved fluorescence spectrum),[20] this is more pronounced in the presence of the phospholipid. β-Phase emission of PFO in films has previously been observed in spin-coated films prepared from PFO solution in *o*-xylene with variable amounts of 1,8-diiodooctene.[22] From the blue shift of the absorption maximum and the weak shoulder of the PFO emission spectrum at 420 nm (characteristic of the emission of random conformation, α-phase) in the absence of DMPC, Figure 4A, it can be concluded that DMPC induces a higher fraction of the ordered β-phase in the films.

To quantify the increase of β-phase formation, a deconvolution was carried out of the absorption spectra as a sum of Gaussians (Figure S4 in Supporting Information). The area of the β-phase Gaussians (at 3.07 and 2.92 eV) represents 12% of the total absorbance in PFO films and 22% for DMPC−PFO ones. These results show that the PFO β-phase is present before the liposome formation in the PFO−DMPC films that give rise to liposome after hydration at the proper temperature with the appropriate treatment detailed in the Experimental Section. It seems that the interaction between PFO and the phospholipid bilayers is the key factor in enhancing the β-phase formation, and the role of the liposome is allowing its formation in aqueous suspension of the whole system at room temperature. This is a significant novelty of this system, since PFO β-phase in solution is normally observed in organic media below room temperature (i.e., in methylcyclohexane (MCH) below 273 K[20,29]).

It is not yet clear exactly how the PFO fits within the phospholipid bilayer. However, molecular dynamics simulations are in progress, and preliminary results with biphenyl as the model compound indicate good solubility within the lipid region with no marked tendency to partition to the interface. NMR and SANS studies of PFO in toluene solution show increasing interchain interactions between alkyl chains on two PFO molecules upon increasing polymer concentration and suggest that this might help stabilize the β-phase.[23] We believe that bilayers act as a template for the PFO molecules. In the preparation of liposomes, the aliphatic chains on one side must locate into the bilayer, interdigitated with the phospolipid alkyl chains. This induces planarization of the polymer backbone stabilizing or directing β-phase formation. On the other hand, the opposite aliphatic chains are in a polar environment. To protect these chains, other PFO molecules can locate themselves on the inserted molecule. A schematic representation of PFO aggregation in the lipid bilayer is shown in Figure S5 (Supporting Information). As we will see in the next section, the effect of PFO on the DMPC phase transition is compatible with this interpretation.

DMPC Phase Transitions. The interaction between PFO and DMPC bilayers can be probed through the changes in phase transitions in both liposomes (DMPC) and solid films (PLTM).

The addition of PFO affects the main DMPC liposome phase transition from an ordered gel to a disordered fluid-like structure. This transition, determined by DSC, occurs at 23.2 °C for pure phospholipids,[30] but upon addition of PFO the peaks of the thermograms are much broader and shift slightly to higher temperatures (+0.5 °C) (Figure 5). Comparable changes previously observed upon addition of fluorinated diblock copolymers, F_nH_m ($F_3C-(CF_2)_{n-1}-(CH_2)_{m-1}-CH_3$), to DMPC vesicles[30] have been attributed to the F_n segments forming a central layer in the

dx.doi.org/10.1021/jp2010666 |*J. Phys. Chem. B* 2011, 115, 5794–5800

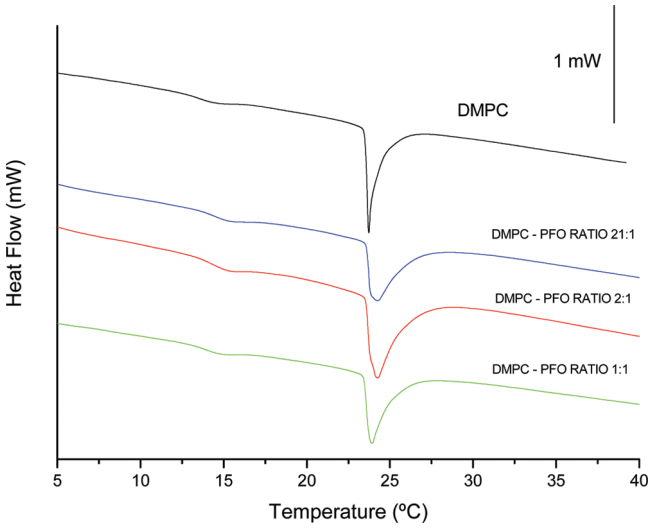

Figure 5. Experimental DSC thermograms for aqueous DMPC (3.69×10^{-2} M) and DMCP−PFO mixtures with DMPC/PFO ratios of 21:1, 2:1, and 1:1, in black, blue, red, and green lines, respectively.

core of the lipid bilayer with the H_m segments interdigitated with the lipid chains.[30] A similar interaction between the octyl chain of the PFO and the DMPC lipid bilayer is likely to be involved in the formation of β-phase in the liposomes. This is in agreement with the conclusion of a spectroscopic study of the influence of the alkyl chain length on β-phase formation in dilute solutions in MCH of polyfluorenes which shows that this phase is formed only if the side chain interactions are stable and sufficient to overcome the steric repulsion and planarize the polymer backbone.[29] This occurs for heptyl, octyl, and nonyl alkyl chains in MCH.[29]

DMPC liposomes correspond to a metastable state relative to the phospholipid−water lamellar L_α liquid crystalline phase. The interaction between DMPC and PFO in films is shown by the PLTM experiments (Figure 6). In the boundary created upon addition of small amounts of water to DMPC films, the formation of lamellar phases occurs,[31,32] and it is reversible in a heating/cooling cycle (Figure 6A). However, when the films contain small amounts of PFO (Figure 6B), the lamellar phase appears only at 45 °C on the heating cycle. At 50 °C some vesicles are formed. The heating/cooling processes are not reversible, and the formation of a ripple phase was observed on cooling at 35 °C, as shown in Figure 6C and as previously described on cooling the lamellar phase of phosphatidylcholine phospholipids.[31,32] At higher concentrations of PFO (Figure 6D), the formation of a new phase is not observed until the system has reached a temperature of 60 °C, and the characteristics are different from the changes described above, showing that, as expected, by increasing the amount of PFO the film becomes more hydrophobic.

Liposome Structure and Size. The effect of PFO addition on the structure and size of DMPC liposomes was studied by TEM and DLS. Both techniques indicate that polydisperse liposomes were obtained (Figures 7 and 8A). The polydispersity index determined by DLS is of 0.43 ± 0.04.

Although, no significant changes in the shape of liposomes could be detected upon addition of PFO (Figure 7), the soft round contours of free liposomes (Figure 7A) seem to adopt

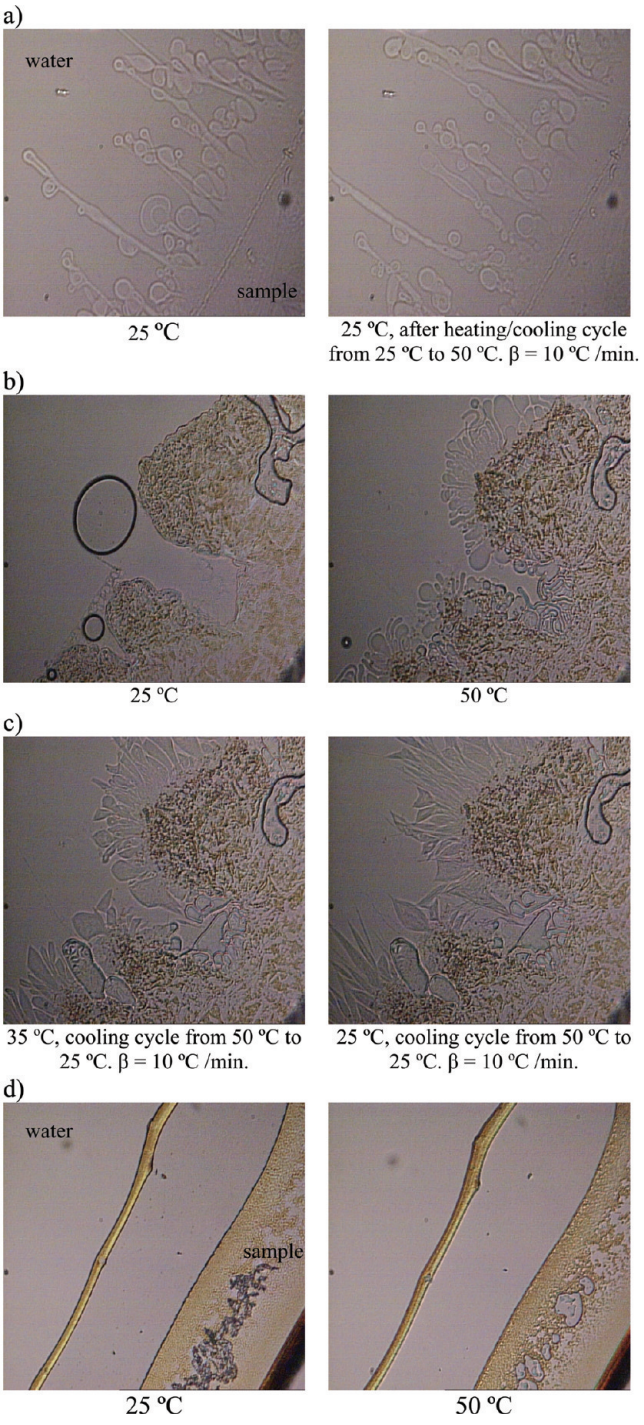

Figure 6. Observation of the boundary between the water and DMPC (2.44×10^{-3} M, 10 μL)/Water (16 μL) sample at 25 °C before heating (left side) and after the heating/cooling cycle from 25 to 50 °C. β = 10 °C/min (right side) (a). DMPC (2.44×10^{-3} M, 10 μL)/PFO (4.80×10^{-4} M, 5 μL)/Water (16 μL) sample heating at 25 and 50 °C (b). Sample of (b) cooling from 50 to 25 °C. β = 10 °C/min (c). DMPC (2.44×10^{-3} M, 10 μL)/PFO (4.80×10^{-4} M, 50 μL)/Water (16 μL) sample on heating from 25 to 50 °C. β = 10 °C/min (d).

slightly more polygonal forms in the presence of the polymer (Figure 7B). In addition, the radius of the liposomes shows a decrease with increasing PFO concentration (Figure 8B).

dx.doi.org/10.1021/jp2010666 |J. Phys. Chem. B 2011, 115, 5794–5800

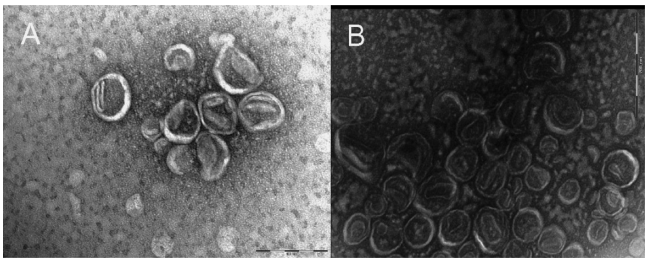

Figure 7. TEM images of (A) aqueous DMPC (1.01×10^{-3} M) and (B) DMPC (1.01×10^{-3} M)−PFO (6.39×10^{-5} M) samples, respectively.

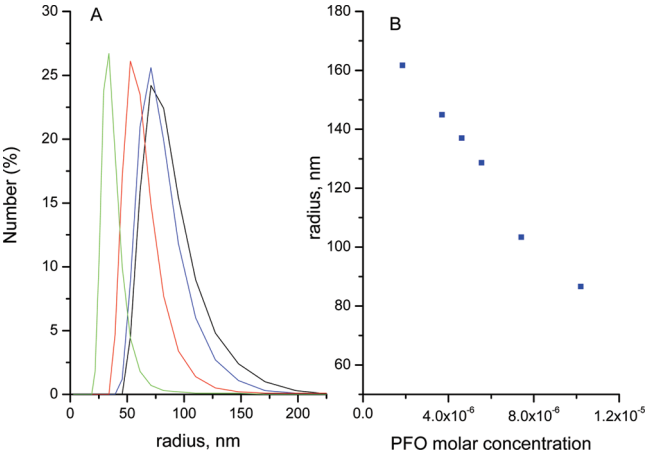

Figure 8. (A) Size distribution curve by number. (B) Change of DMPC liposome radius as a function of PFO molar concentration. DMPC (9.35×10^{-5} M) and PFO: 0 (black line), 2.78×10^{-6} (blue line), 4.63×10^{-6} (red line), and 9.26×10^{-6} M (green line).

CONCLUSIONS

PFO can be solubilized in DMPC phospholipid bilayers, either as polydisperse aqueous liposomes or as the lamellar phase in thin films. This leads to the well-structured β-phase PFO emission. The percentage of β-phase increases with the number of polymer chains per liposome showing that polymer−polymer interactions are probably involved in the formation of β-phase which explains the loss of anisotropy of these systems. Although the β-phase is observed in PFO films, its percentage is nearly doubled by the presence of DMPC in the film. The polymer−phospholipid interaction in the solid state leads to films that cannot easily hydrate and in liposomes leads to a slight increase (0.5 °C) in the gel to fluid transition temperature. This supports the role of alkyl chain interactions in the stabilization of this phase and provides a novel route to β-phase formation in aqueous dispersions at room temperature. Polydisperse liposomes (radius <200 nm) were obtained whose shape is hardly affected by the presence of the polymer but whose radius tends to decrease with PFO concentration. This provides the potential of the PFO β-phase incorporated in the liposomes providing structural information on their phospholipid bilayers, possibly by using amplified fluorescence quenching or energy transfer.[33]

ASSOCIATED CONTENT

Supporting Information. Changes in PFO absorption and emission intensities with polymer concentration. Dependence of the PFO β-phase with the number of polymer chains per liposome. Anisotropy. Deconvolution of absorption spectra of PFO in films. A schematic representation of PFO aggregation in the lipid bilayer. This material is available free of charge via the Internet at http://pubs.acs.org.

AUTHOR INFORMATION

Corresponding Author

*María José Tapia. E-mail: mjtapia@ubu.es. Phone: +34 947258061. Fax: (+34) 947 28831. Hugh D. Burrows. E-mail: burrows@ci.uc.pt. Phone: +351 239854482. Fax: (+351) 239 827703.

ACKNOWLEDGMENT

MEC and FEDER are thanked for financial support through the MAT2008-06079/MAT. Funding from the European Community's Seventh Framework Programme under grant agreement n° 228334 is acknowledged. Thanks are due to the Foundation for Science and Technology (FCT-Portugal) for financial support and for a postdoctoral grant to J.P. (SFRH/BPD/65507/2009).

REFERENCES

(1) Zainelabdin, A.; Zaman, S.; Amin, G.; Nur, O.; Willander, M. *Nanoscale Res. Lett.* **2010**, *5*, 1442.
(2) Chun-Yuan, H.; Tsung-Syun, H.; Chiao-Yang, C.; Ying-Chih, C.; Cheng-Tien, W.; Rao, M. V. M.; Yan-Kuin, S. *Photonics Technol. Lett., IEEE* **2010**, *22*, 305.
(3) Guo, X.; Cheng, Y.; Xie, Z.; Geng, Y.; Wang, L.; Jing, X.; Wang, F. *Macromol. Rapid Commun.* **2009**, *30*, 816.
(4) Levermore, P. A.; Jin, R.; Wang, X.; de Mello, J. C.; Bradley, D. D. C. *Adv. Funct. Mater.* **2009**, *19*, 950.
(5) Giovanella, U.; Pasini, M.; Destri, S.; Porzio, W.; Botta, C. *Synth. Met.* **2008**, *158*, 113.
(6) Sun, M.; Wang, L.; Yang, W. *J. Appl. Polym. Sci.* **2010**, *118*, 1462.
(7) Wang, E.; Wang, M.; Wang, L.; Duan, C.; Zhang, J.; Cai, W.; He, C.; Wu, H.; Cao, Y. *Macromolecules* **2009**, *42*, 4410.
(8) Zhou, Q. M.; Hou, Q.; Zheng, L. P.; Deng, X. Y.; Yu, G.; Cao, Y. *Appl. Phys. Lett.* **2004**, *84*, 1653.
(9) Ryu, G.; Stavrinou, P. N.; Bradley, D. D. C. *Adv. Funct. Mater.* **2009**, *19*, 3237.
(10) Stavrinou, P. N.; Ryu, G.; Campoy-Quiles, M.; Bradley, D. D. C. *J. Phys.: Condens. Matter* **2007**, *19*, 14.
(11) Qualtieri, A.; Stomeo, T.; Lattante, S.; Anni, M.; Martiradonna, L.; De Vittorio, M. *Microelectron. Eng.* **2007**, *84*, 1581.
(12) Rothe, C.; Galbrecht, F.; Scherf, U.; Monkman, A. *Adv. Mater.* **2006**, *18*, 2137.
(13) Rabe, T.; Hoping, M.; Schneider, D.; Becker, E.; Johannes, H. H.; Kowalsky, W.; Weimann, T.; Wang, J.; Hinze, P.; Nehls, B.; Scherf, U.; Farrell, T.; Riedl, T *Adv. Funct. Mater.* **2005**, *15*, 1188.
(14) Heliotis, G.; Xia, R.; Turnbull, G.; Andrew, P.; Barnes, W.; Samuel, I.; Bradley, D. *Adv. Funct. Mater.* **2004**, *14*, 91.
(15) Heliotis, G.; Xia, R.; Whitehead, K. S.; Turnbull, G. A.; Samuel, I. D. W.; Bradley, D. D. C. *Synth. Met.* **2003**, *139*, 727.
(16) Heliotis, G.; Bradley, D. D. C.; Turnbull, G. A.; Samuel, I. D. W. *Appl. Phys. Lett.* **2002**, *81*, 415.
(17) Winokur, M. J.; Slinker, J.; Huber, D. L. *Phys. Rev. B* **2003**, *67*, 184106.
(18) Chunwaschirasiri, W.; Tanto, B.; Huber, D. L.; Winokur, M. J. *Phys. Rev. Lett.* **2005**, *94*, 107402.
(19) Rodrigues, R. F.; Charas, A.; Morgado, J.; Maçanita, A. L. *Macromolecules* **2010**, *43*, 765.
(20) Dias, F. B.; Morgado, J.; Maçanita, A. L.; da Costa, F. P.; Burrows, H. D.; Monkman, A. P. *Macromolecules* **2006**, *39*, 5854.

(21) Da Como, E.; Becker, K.; Feldmann, J.; Lupton, J. M. *Nano Lett.* **2007**, *7*, 2993.
(22) Peet, J.; Brocker, E.; Xu, Y.; Bazan, G. C. *Adv. Mater.* **2008**, *20*, 1882.
(23) Justino, L. L. G.; Knaapila, M.; Ramos, M. L.; Marques, A. T.; Kudla, C.; Almásy, L.; Schweins, R.; Scherf, U.; Burrows, H. D.; Monkman, A. *Macromolecules* **2011**, *44*, 334.
(24) Pina, J.; Seixas de Melo, J.; Burrows, H. D.; Maçanita, A. L.; Galbrecht, F.; Buinnagel, T.; Scherf, U. *Macromolecules* **2009**, *42*, 1710.
(25) Striker, G.; Subramaniam, V.; Seidel, C. A. M.; Volkmer, A. J. *J. Phys. Chem. B* **1999**, *103*, 8612.
(26) Lakowicz, J. R. *Principles of Fluorescence Spectroscopy*, 2nd ed.; Kluwer Academic/Plenum Publishers: New York, 2004.
(27) Mallavia, R.; Paya, F. J.; Salinas, A.; Estepa, A.; Mateo, C. R. *Bioeng. Bioinspired Syst. III* **2007**, *6592*, 59213.
(28) Vaughan, H. L.; Dias, F. M. B.; Monkman, A. P. *J. Chem. Phys.* **2005**, *122*, 014902.
(29) Bright, D. W.; Dias, F. B.; Galbrecht, F.; Scherf, U.; Monkman, A. P. *Adv. Funct. Mater.* **2009**, *19*, 67.
(30) Sabín, J.; Prieto, G.; Estelrich, J.; Sarmiento, F.; Costas, M. *J. Colloid Interface Sci.* **2010**, *348*, 388.
(31) Sengupta, K.; Raghunathan, V. A.; Katsaras, J. *Phys. Rev. E* **2003**, *68*, 031710.
(32) Meyer, H. W.; Richter, W. *Micron* **2001**, *32*, 615.
(33) Thomas, S. W.; Joly, G. D.; Swager, T. M. *Chem. Rev.* **2007**, *107*, 1339.